

Biochemical analysis of the Cas6-1 RNA endonuclease associated with the subtype I-D CRISPR-Cas system in *Synechocystis* sp. PCC 6803

Rabea Jesser, Juliane Behler, Christian Benda, Viktoria Reimann & Wolfgang R. Hess

To cite this article: Rabea Jesser, Juliane Behler, Christian Benda, Viktoria Reimann & Wolfgang R. Hess (2018): Biochemical analysis of the Cas6-1 RNA endonuclease associated with the subtype I-D CRISPR-Cas system in *Synechocystis* sp. PCC 6803, RNA Biology, DOI: [10.1080/15476286.2018.1447742](https://doi.org/10.1080/15476286.2018.1447742)

To link to this article: <https://doi.org/10.1080/15476286.2018.1447742>



Accepted author version posted online: 08 Mar 2018.
Published online: 26 Mar 2018.



Submit your article to this journal [↗](#)



Article views: 89



View Crossmark data [↗](#)

RESEARCH PAPER



Biochemical analysis of the Cas6-1 RNA endonuclease associated with the subtype I-D CRISPR-Cas system in *Synechocystis* sp. PCC 6803

Rabea Jesser^{a*}, Juliane Behler^{a*}, Christian Benda^b, Viktoria Reimann^a, and Wolfgang R. Hess^{id a,c}

^aGenetics and Experimental Bioinformatics, Faculty of Biology, University of Freiburg, Schänzlestr. 1, Freiburg, Germany; ^bDepartment of Structural Cell Biology, Max-Planck-Institute of Biochemistry, Am Klopferspitz 18, Martinsried, Germany; ^cFreiburg Institute for Advanced Studies, University of Freiburg, Albertstr. 19, Freiburg, Germany

ABSTRACT

Specialized RNA endonucleases are critical for efficient activity of the CRISPR-Cas defense mechanisms against invading DNA or RNA. Cas6-type enzymes are the RNA endonucleases in many type I and type III CRISPR-Cas systems. These enzymes are diverse and critical residues involved in the recognition and cleavage of RNA substrates are not universally conserved. Cas6 endonucleases associated with the CRISPR-Cas subtypes I-A, I-B, I-C, I-E and I-F, as well as III-B have been studied from three archaea and four bacteria thus far. However, until now information about subtype I-D specific Cas6 endonucleases has remained scarce. Here, we report the biochemical analysis of Cas6-1, which is specific for the crRNA maturation from the subtype I-D CRISPR-Cas system of *Synechocystis* sp. PCC 6803. Assays of turnover kinetics suggest a single turnover mechanism for Cas6-1. The mutation of conserved amino acids R29A, H32A-S33A and H51A revealed these as essential, whereas the parallel mutation of R175A-R176A led to a pronounced and the K155A mutation to a slight reduction in enzymatic activity. In contrast, the mutations R67A, R81A and K231A left the enzymatic activity unchanged. These results are in accordance with the predominant role of histidine residues in the active site and of positively charged residues in RNA binding. Nevertheless, the protein-RNA interaction site seems to differ from other known systems, since imidazole could not restore the mutated histidine site.

ARTICLE HISTORY

Received 12 December 2017
Accepted 28 February 2018

KEYWORDS

Cas6; CRISPR; cyanobacteria;
RNA endonuclease; RNA
maturation

Introduction

Clustered Regularly Interspaced Short Palindromic Repeats (CRISPR) and CRISPR-associated (Cas) proteins provide an adaptable and inheritable immune system against viruses and other foreign genetic elements [1–4]. CRISPR-based immunity relies on the transcription of a repeat-spacer array, ultimately leading to short CRISPR RNAs (crRNAs) that guide the CRISPR complexes in the recognition and destruction of invading nucleic acids. CRISPR-Cas loci have been categorized into two major classes, six major types I–VI and into at least 19 subtypes [5–8]. In type I, III, V and VI CRISPR-Cas systems longer crRNA precursor transcripts are processed by an endoribonuclease into crRNAs of 70–80 nt in length and, in some type I and III systems, in a second ribonucleolytic step into even shorter mature crRNAs of 40–50 nt [9–12]. The known endoribonucleases in most type I and III systems belong to the Cas6 family of proteins, whereas Cas5d is the endoribonuclease in subtype I-C systems [13,14]. In contrast, Cas12a (previously known as Cpf1), a single effector enzyme, mediates the pre-crRNA processing in subtype V-A [15] and Cas13a (previously known as C2c2) in subtype VI systems [16].

Cas6 endoribonucleases are extremely divergent, which, in part may be related to their high specificity. Nevertheless, Cas6

enzymes from one organism that share about 20% identical amino acid residues can process identical repeat substrates, at least *in vitro* [17]. It is only partially understood how the highly diverse Cas6 endoribonucleases perform a common function – endoribonucleolytic cleavage – but differentiate between their different targets – especially in organisms with multiple CRISPR systems [5]. Facts such as these have triggered interest in studying Cas6 enzymes more closely. Crystal structures or the function of particular residues was previously studied for eight different Cas6 enzymes and one Cas5d protein. These proteins belong to seven different archaea and bacteria. In case of archaea, these enzymes were Cas6-1A and Cas6-1B (SSO2004 and SSO1437) from *Sulfolobus solfataricus* [18–20] MmCas6b from *Methanococcus maripaludis* [21] and PfCas6 from *Pyrococcus furiosus* [22]. The bacterial enzymes are Cas6e of *Escherichia coli* [23,24], Cas6f of *Pseudomonas aeruginosa* [25,26] and Cas6A and Cas6B from *Thermus thermophilus* [27]. The Cas5d protein was studied from *Bacillus halodurans* [13]. These enzymes are associated with the CRISPR-Cas subtypes I-A, I-B, I-C, I-E and I-F, as well as III-B. However, no subtype I-D specific Cas6 endonuclease nor any enzyme from the cyanobacterial phylum has been studied so far.

In the cyanobacterium *Synechocystis* sp. PCC 6803 three separate CRISPR-Cas systems are encoded on the large plasmid

pSYSA [28]. Based on genetic evidence, the associated endoribonucleases, Cas6-1, Cas6-2a and Cas6-2b, were determined to be involved in crRNA maturation from two of these systems, which were classified as subtype I-D and subtype III-D CRISPR-Cas systems, respectively [28]. In contrast, crRNA maturation in the third system, classified as subtype III-Bv, is independent of any Cas6 activity and instead proceeds through the major housekeeping riboendonuclease E [29].

The deletion of the *cas6-1* gene (*slr7014*) abolished the accumulation of crRNAs, processing intermediates and precursors for the subtype I-D CRISPR-Cas system [28] consistent with a function of Cas6-1 as its maturation endoribonuclease that was also confirmed by experiments *in vitro* [17]. With the here presented work, we aim at the specific cleavage mechanism of Cas6-1, its active site and RNA binding interface.

Results

Comparison of Cas6-1 to other enzymes of this class

Cas6-1 was compared in multiple amino acid sequence alignments separately to cyanobacterial Cas6 proteins, and to previously studied Cas6 enzymes and the Cas5d enzyme (Fig. 1; Fig. S1). The most closely related protein is the Cas6 protein of the cyanobacterium *Synechococcus* sp. PCC 7002 encoded by gene *SYNPCC7002_D0021* on plasmid pAQ4 (71.15% identical residues). The most remote CRISPR riboendonuclease that can be aligned is Cas5d of *Bacillus halodurans* with only 11.5% identical residues. The percentage of identical residues with most previously characterized Cas6 proteins is in between ~15% for the *Sulfolobus solfataricus* Cas6-1A, Cas6-1B and Cas6-3 enzymes, 29% and 26% for the *Thermus thermophilus* Cas6A and Cas6B proteins, or 21% for the *Pseudomonas aeruginosa* Cas6f enzyme. However, some proteins, such as Cas6e of *Escherichia coli* [23,24], or Csy4 of *Pectobacterium atrosepticum* [12] are too remote and cannot be compared in pairwise sequence alignments. Despite the low general sequence identity, the previously described glycine-rich-loop (G-loop) is conserved in the very C-terminal region (Fig. 1). This loop is located between $\alpha 4$ and the last β strand, $\beta 8$, at the interface between two ferredoxin-like folds [30]. Several other conserved amino acid residues cluster in the N-terminal part of the aligned Cas6 proteins (Fig. 1) and comprise, among others, mainly positively charged amino acids like histidine, lysine or arginine residues, which hence are candidates to be involved in RNA-protein interactions or functions in the catalytic center.

Biochemical analyses of mutagenized versions of Cas6-1 endonucleases *in vitro* and *in vivo*

Based on the amino acid sequence comparison shown in Fig. 1 and Fig. S1, ten residues were selected for the exchange of the native amino acid to alanine (R29, H32, S33, H51, R67, R81, K155, R175, R176, K231). Directly adjacent amino acids (H32-S33, R175-R176) were replaced together, hence eight different Cas6-1 mutant proteins were generated. After overexpression and purification of the recombinant proteins from *E. coli* (Fig. 2A), their activity was analyzed *in vitro*. Cleavage assays were conducted both with a synthetic CRISPR1 RNA repeat

oligonucleotide (Fig. 2B) and a longer substrate, an *in vitro* generated synthetic CRISPR1 precursor RNA (Fig. 2C). This longer substrate encompasses two artificial spacers with a length of 36 nt because native CRISPR1 spacers vary between 31 and 41 nucleotides in size [31]. Upon proper maturation, two artificial CRISPR RNAs (acrRNAs) would derive from this transcript.

Reactions containing Cas6-1 wild-type protein (Cas6-1 WT) exhibited a distinct cleavage pattern, whereas the substrates remained intact in mock incubations and the other negative controls (Fig. 2B, C). The CRISPR1 repeat oligonucleotide was shortened by Cas6-1 WT from 37 nt to 29 nt, which corresponds precisely to the 8 nt removed also *in vivo* [28]. Based on the mapped cleavage site of Cas6-1 within the CRISPR1 repeat sequence [28], predictable cleavage intermediates could be assigned also to almost every other detected signal. Only the 39 nt fragment obtained with the longer substrate and corresponding to the *oop* terminator, was degraded further, which underscores the stability of the other RNA fragments (Fig. 2C). Comparing the cleavage activity between Cas6-1 WT and mutant versions, striking variation was observed. The three variants R67A, R81A and K231A with substitutions in amino acid positions highly conserved among cyanobacterial Cas6 proteins (Fig. S1A) yielded cleavage products of the same lengths as produced by Cas6-1 WT. Thus, these residues do not seem to play a role in enzymatic activity or RNA binding at all, but due to their conservation they might have other conserved functions (e.g., binding of adaptor proteins). On the contrary, substitution of one histidine residue – H51 – eliminated cleavage activity, suggesting its potential participation in the active site. The substitution of one – R29 – or two other amino acid residues – H32-S33 – interfered almost completely with processing. Thus, these residues play an important role either in the enzymatic reaction or in binding of the RNA substrate. Mutations of K155 and R176-R177 considerably affected Cas6-1 enzymatic activity but did not abolish it completely. Therefore, they might affect RNA binding or the Cas6-1 active site but to a lesser extent than R29, H32-S33. In addition, the appearance of weak additional bands in case of the R29A, K155A and H51A variants indicated a relaxed target recognition in case of the longer substrate (Fig. 2C).

The presence of the other Cas proteins and additional factors may influence the enzyme kinetics or specificity of Cas6-1. To test this possibility directly, the genes of the WT Cas6-1 and six variant enzymes were transformed into a CRISPR1 knock-out deletion strain. Since R67A, R81A and K231A did not show any effects on Cas6-1 processing activity, we continued *in vivo* Cas6-1 analyses exemplary only with one of the mutated Cas6-1 variants – R67A. Transcription of *cas6-1* WT and mutant variants was controlled via the copper-inducible *petE* [32,33] promoter. The pre-acrRNA used as the longer substrate in Fig. 2C was in this case expressed *in trans* from the plasmid vector pVZ321 under the control of the zinc-inducible *zlaA* [34] promoter. Strains expressing Cas6-1 WT showed reduced pre-acrRNA accumulation in the presence of both inducers due to its processing by catalytically active Cas6-1 into intermediates of different lengths (Fig. 3). The smallest fragment derived from the pre-acrRNA was a 73 nt long intermediate (marked with asterisks) that was only detectable in the Cas6-1 WT and the R67A mutant. Thus, the R67A mutant showed comparable

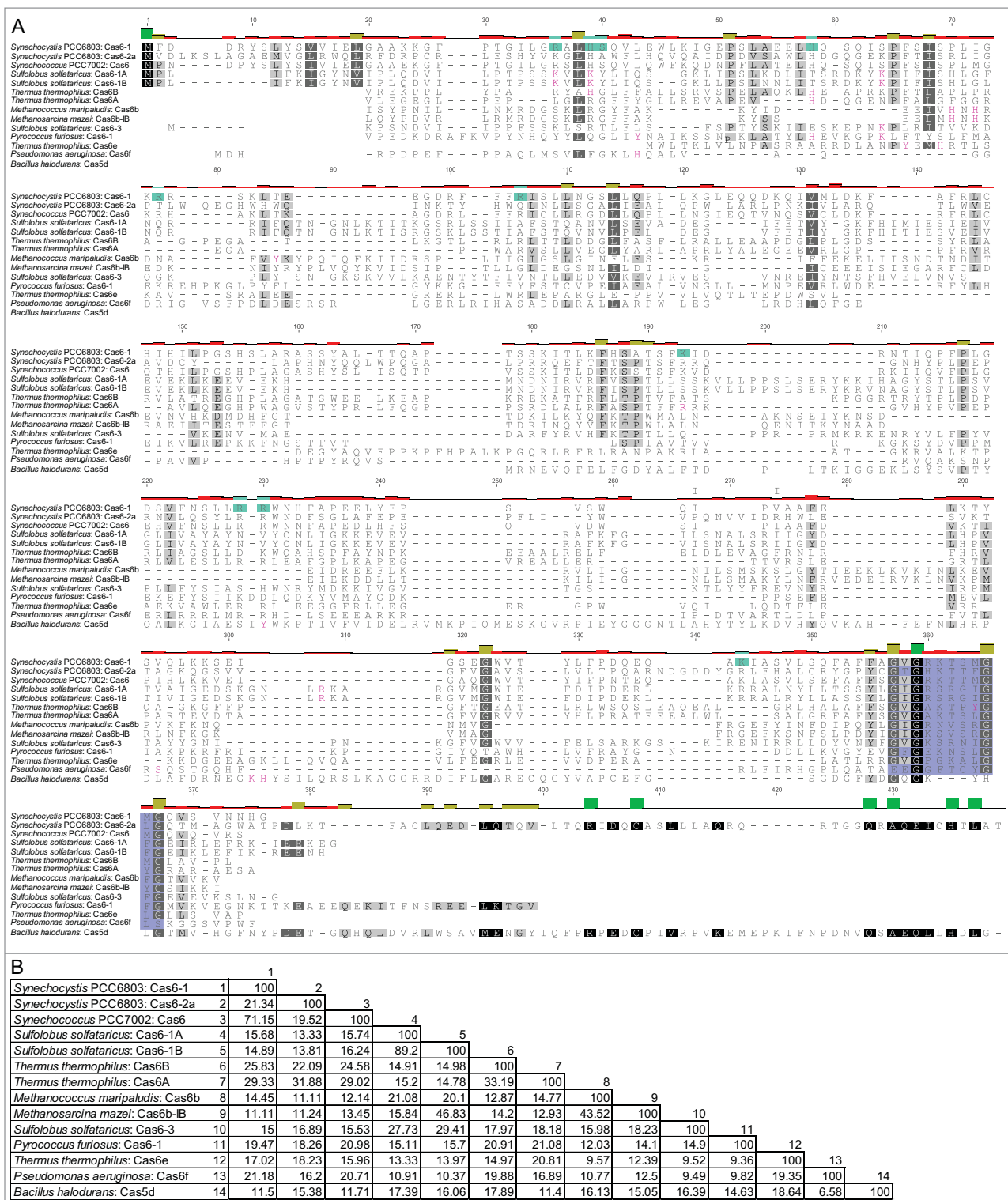


Figure 1. Multiple amino acid sequence alignment and identity matrix of *Synechocystis* Cas6-1 and Cas6-2a and the crRNA processing enzymes of different bacteria and archaea. (A) Multiple sequence alignments visualize the tremendous sequence diversity within the Cas6 and Cas5d protein families. Different degrees of conservation among the compared sequences is indicated by different grey shading of the respective amino acid residues and colored boxes above the alignment (red: low; ochre: medium; green: high degree of conservation). Residues that were selected for site directed mutagenesis are highlighted in turquoise. Magenta points to published active site residues. The Cas6 glycine-rich loop (G-loop) is boxed in dark blue. Protein sequences are available in the NCBI protein database with the following IDs: Q97WV8 (*Sulfolobus solfataricus*: Cas6-1A), Q97Y96 (*Sulfolobus solfataricus*: Cas6-1B), Q6ZIE4 (*Synechocystis* PCC 6803: Cas6-1), B1XQV2 (*Synechococcus* PCC 7002: Cas6), WP_024118777 (*Thermus thermophilus*: Cas6B), WP_024118933 (*Thermus thermophilus*: Cas6A), YP_001097292 (*Methanococcus maripaludis*: Cas6b), AKB60698 (*Methanosarcina mazei*: Cas6b-B), AKA79869 (*Sulfolobus solfataricus*: Cas6-3), BAD01970.1 (*Synechocystis* PCC 6803: Cas6-2a), Q8U1S4 (*Pyrococcus furiosus*: Cas6-1), Q53WG9 (*Thermus thermophilus*: Cas6e), BAO39804 (*Pseudomonas aeruginosa*: Cas6f), WP_010896518 (*Bacillus halodurans*: Cas5d). (B) Identity matrix of aligned crRNA maturation ribonucleases from panel (A). Sequence identities between the different proteins range between 6.58% and 71.15%. Numbers (1 to 14) associated with the different strains vertically correspond to the horizontal numbers. Sequence identity is represented in percent.

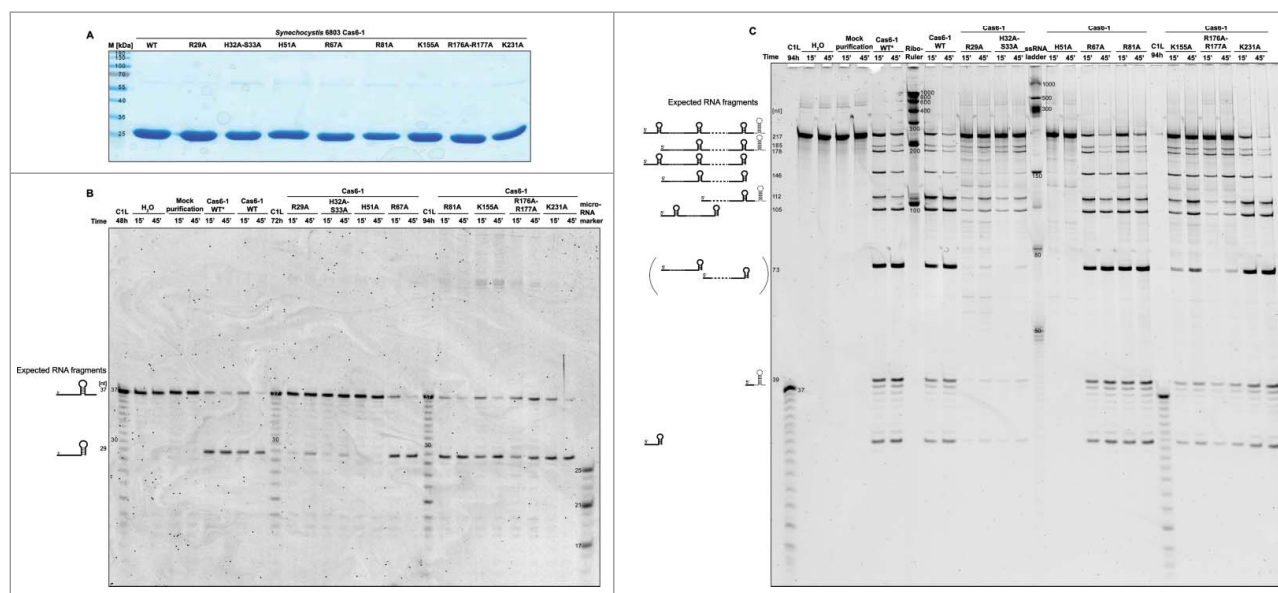


Figure 2. Purification and *in vitro* cleavage assay of *Synechocystis* WT Cas6-1 and mutated Cas6-1 proteins. (A) Coomassie-stained 15% SDS-PAGE of heterologously over-expressed and purified Cas6-1 protein variants. The expected molecular weight of Cas6-1_{6xHis} is ~ 30 kDa. 66.67 pmol recombinant enzyme was loaded on each lane and PageRuler™ Prestained Protein Ladder (Thermo Fisher Scientific) served for protein size estimation. (B, C) *In vitro* cleavage assays both the (B) CRISPR1 RNA oligo repeat sequence and the (C) pre-acrRNA cassette is processed with variable efficiency by the purified Cas6-1 protein variants shown in (A). After incubation at 30°C the RNA fragments were electrophoretically size separated on a 15% PAA sequencing gel and visualized with SYBR® Gold Nucleic Acid Gel Stain. The processing results in a pattern of RNA fragments of distinct lengths. Cleavage assays were conducted with a three-fold excess (B) or a 1:1 ratio (C) of protein to RNA-substrate in cleavage buffer and incubated at 30°C for the indicated time. Expected RNA fragments and their corresponding sizes are illustrated by cartoons. Another Cas6-1 WT protein sample, which was overexpressed and purified independently, is indicated by an asterisk. Negative controls were complemented with 1 μ L of H₂O or 1 μ L eluate of a mock control. Two additional nucleotides resulting from *in vitro* transcription were added to the 215 nt long acrRNA yielding a 217 nt long pre-acrRNA. For RNA size estimation a CRISPR1 repeat oligo ladder (C1L), RiboRuler low range RNA ladder (Thermo Fisher Scientific), low range ssRNA ladder or microRNA marker (both from New England Biolabs) were used.

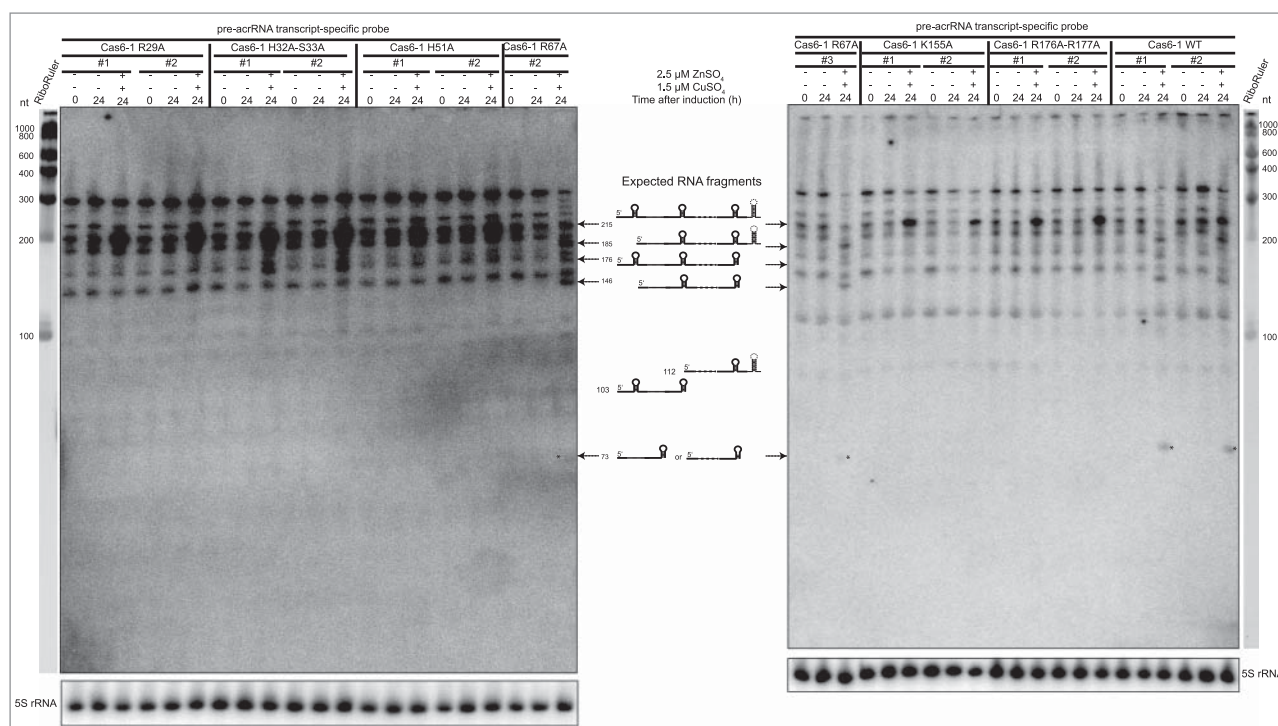


Figure 3. *In vivo* cleavage assay of Cas6-1 protein variants and pre-acrRNA. Northern Blot analysis using a radioactively labeled transcript probe spanning the entire pre-acrRNA cassette. The RiboRuler low range RNA ladder was used as a size marker. Cas6-1 expression was controlled by the copper inducible *petE* promoter [32,33], whereas acrRNA was zinc inducible by the *ziaA* promoter [34]. The smallest detectable processing intermediate of 73 nt in size is marked by asterisks. WT Cas6-1 and the R67A protein variant show comparable cleavage performance indicating that R67A is not involved in the active site or RNA binding of the enzyme. In contrast, the remaining mutated proteins show distinct acrRNA accumulation and lack acrRNA derived cleavage intermediates.

enzyme activities as the WT enzyme *in vivo* as well as *in vitro* (Fig. 2B, C). In contrast, the mutated variants R29A, H32A-S33A, H51A, K155A and R176A-R177A exhibited strong pre-acrRNA accumulation and further processing intermediates were not detectable indicating strongly abolished functionality *in vivo*. Therefore, the Cas6-1 H51A mutant was found dysfunctional both *in vivo* and *in vitro*, whereas the R29A, H32A-S33A, K155A and R176A-R177A protein variants were dysfunctional *in vivo* but displayed some enzymatic activity *in vitro*. In addition to the expected full-length and processed acrRNAs, fragments of higher and lower molecular mass were only detected in strains containing the acrRNA encoding conjugative plasmid pVZ321 and did not result from the strain itself (Fig. S2). These additional fragments originate from an alternative transcriptional start site located upstream of the acrRNA encoding locus and are therefore of unspecific origin.

Cas6-1 is a single turnover endonuclease

Up to this point, no data were available whether *Synechocystis* 6803 Cas6-1 operates in single or multiple turnover mode. To clarify this, cleavage assays with different enzyme to substrate molar ratios (1:1, 1:2, 1:4 and 1:8) were conducted with Cas6-1 WT (Fig. 4A). The percentage of cleaved RNA was determined for each reaction and plotted against time (Fig. 4B). While the enzyme concentration was kept constant, increasing substrate amounts led to a similar proportional decrease in the percentage of cleaved RNA. Thus, Cas6-1 acts in single turnover mechanism. Furthermore, most of the substrate (~70%) was processed within the first 60 minutes and the velocity of the reaction slowed down within the following 60 minutes, indicating that saturation was reached. To allow the comparison with other characterized CRISPR maturation enzymes the rate of cleavage was determined. Therefore, cleavage assays were performed with excess of Cas6-1 over CRISPR1 repeat with different molar ratios (2:1, 4:1 and 8:1). The decrease of uncleaved substrate was monitored over time for 15 min (Fig. S3A) and was plotted against time in an exponential decay curve (Fig. S3B). To determine the cleavage rate constant k_{cl} the natural logarithm of the fraction of the remaining substrate was plotted against time whereas the slope of the line corresponds to $-k_{cl}$ (Fig. S3C). All experiments were performed in triplicates and the determined cleavage rate k_{cl} for Cas6-1 was, on average, for a 2:1 enzyme to substrate ratio 0.0412 min^{-1} with a standard error of the mean (SEM) of ± 0.0023 . For a 4:1 and 8:1 ratio, we found $k_{cl} = 0.0521 \pm 0.0018 \text{ min}^{-1}$ and $k_{cl} = 0.0627 \pm 0.0011 \text{ min}^{-1}$, respectively.

Imidazole is incapable to restore endonuclease activity of the inactive Cas6-1 H51A mutant

In vitro and *in vivo* cleavage assays highlighted an important role of the histidine on position 51 in Cas6-1 cleavage efficiency. In previous studies, addition of imidazole – as a histidine mimic – to the cleavage buffer could compensate a mutated active-site histidine [27,35]. To test whether this is also possible for the catalytically impaired Cas6-1 H51A mutant, 500 mM imidazole was added to the cleavage buffer as described by Niewoehner et al. [27]. The reactions were either

pre-incubated without enzyme at 4°C overnight, then supplemented with enzyme and incubated at 30°C, or directly incubated at 30°C. Neither procedure could recover Cas6-1 cleavage activity in the H51A mutant indicating different biochemical properties of the tested enzyme in comparison to previously investigated Cas6 enzymes (Fig. 5).

CRISPR repeat sequence comparison and mapping of Cas6-1-repeat RNA co-structures

To facilitate mapping of the here investigated residues in Cas6-1 to a structural model we chose the *Sulfolobus solfataricus* Cas6-1A (SsCas6) cocrystal structure in complex with the cognate repeat RNA [19]. Pairwise nucleotide alignments of the *S. solfataricus* CRISPR repeat with the *Synechocystis* 6803 CRISPR1 repeat revealed a sequence identity of 66.67% in a 24 nt long overlap. Both repeats share the presence of a five nt long loop on top of a predicted stem-loop secondary structure [19,28]. However, while this structure includes four G-C base pairs in the *Synechocystis* 6803 CRISPR1 repeat and therefore appears energetically strong (Fig. 6A), Cas6-1A is required for stabilization of a relatively weak three nt stem-loop structure [19]. Nonetheless, we decided to use the *S. solfataricus* repeat RNA cocrystal structure for PyMol analysis of *Synechocystis* 6803 Cas6-1. Taking a closer look at the model, it is striking that those amino acids whose modification had an impact on Cas6-1 catalytic activity *in vitro* and *in vivo* (R29A, H32A-S33A, H51A, K155A, R176A-R177A, shown in green) are positioned in close proximity to the repeat RNA suggesting a role of these residues in the active site catalyzing either RNA binding or substrate cleavage (Fig. 6B, C). The other residues (R67A tested *in vivo* and *in vitro*, R81A and K231A only tested *in vitro*, shown in orange) revealed no effect on the Cas6-1 activity and are located distant from the repeat RNA indicating that these residues are not involved in the active site of the enzyme. Likewise, it stands out that the G-loop is also part of a potential RNA-binding pocket surrounded by the residues establishing the catalytic site of the enzyme.

Discussion

Cas6 enzymes are critical for the maturation of crRNA in most type I and III CRISPR-Cas systems. These endoribonucleases are very divergent, which might correlate with high substrate specificity. Here, we show that cyanobacterial Cas6 proteins vary from ~20-70% in sequence identity. Cas6 endoribonucleases have been characterized for several bacterial and archaeal species. These previously characterized Cas6 enzymes plus Cas5d, were used for multiple amino acid sequence alignments to identify conserved residues that are potentially involved in the catalytic site or RNA binding capability of *Synechocystis* Cas6-1. Here, we investigated eight mutated Cas6-1 proteins *in vitro* and six *in vivo*. The mutation H51 was found to be sufficient to completely abolish Cas6-1 endonuclease activity either by destroying the catalytic site or RNA binding capability. High occurrence of histidine residues taking part in the active site was reported for several Cas6 enzymes of various species [6,25–27,36,37]. The remaining Cas6-1 protein variants exhibited either unchanged or reduced Cas6-1 activity of

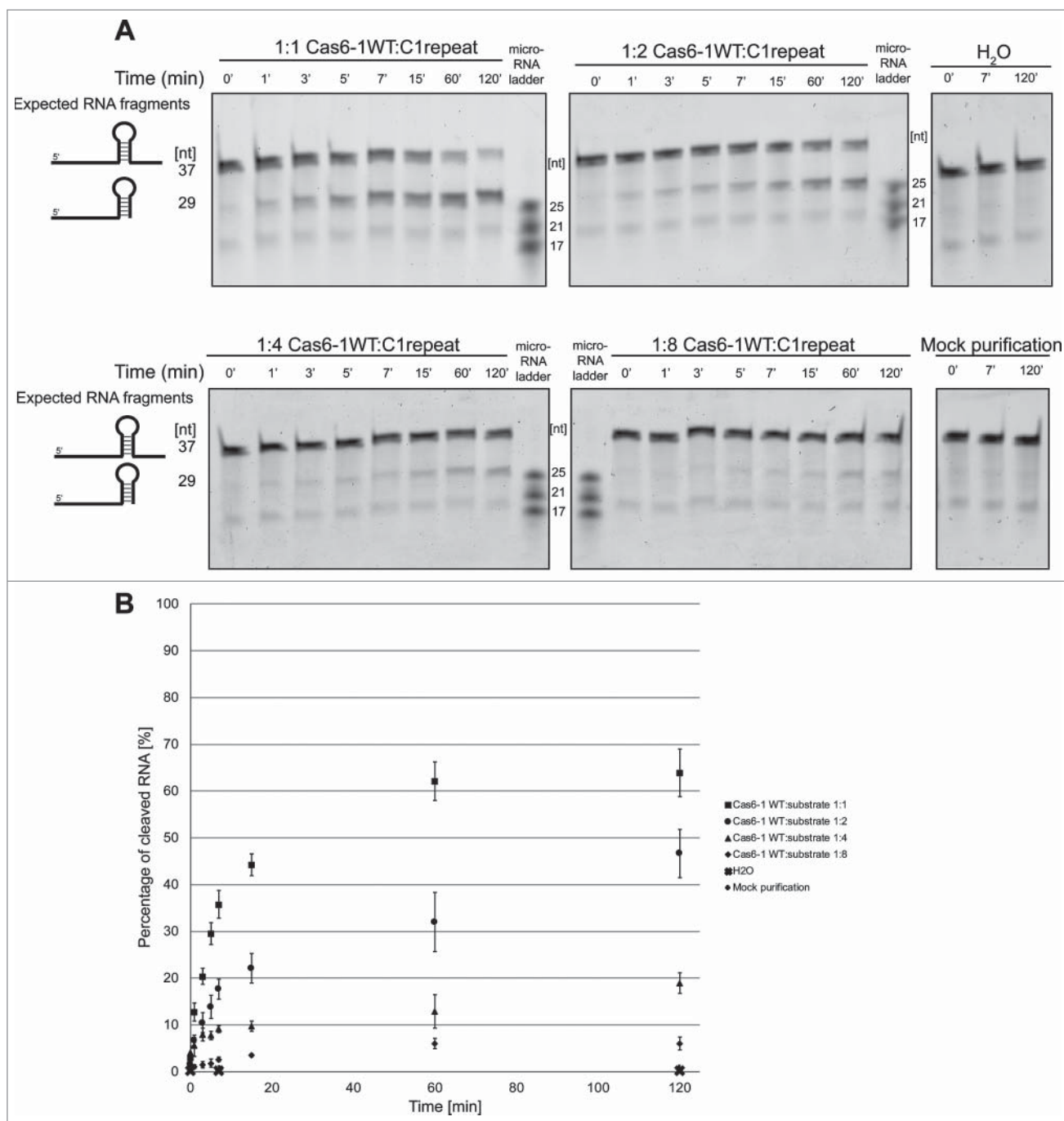


Figure 4. *In vitro* cleavage assays of Cas6-1 WT reveals a single turnover mechanism. *In vitro* cleavage assays with varying enzyme to substrate (CRISPR1 repeat RNA oligo) ratios revealed a single turnover mechanism for the WT Cas6-1. Protein to RNA ratios were applied as indicated above the respective image. RNA cleavage was visualized on a SYBR® Gold stained 15% PAA gel and analyzed with Quantity One software (BIO-RAD). Negative controls were complemented with 1 μ L of H₂O or 1 μ L eluate of a mock control. The low molecular weight band of ~20 nt visible in all lanes is a synthesis by-product. The microRNA marker (New England Biolabs) served for RNA size estimation. (B) ImageJ was used to calculate the percentage of cleaved RNA from the gel images by the amount of product divided by the sum of the amount of product and substrate multiplied by 100 and plotted against time. Standard errors of the mean (SEM) are indicated by vertical bars. A representative of three independent replicates is shown.

different extent. However, the residues showing no effect on Cas6-1 activity are highly conserved among Cas6 enzymes of different species pointing to an alternative function, e.g., in protein folding, maintenance of protein structure or binding sites for other molecules, e.g., adaptor proteins.

Cas6-1 seems to have a histidine based active site or RNA binding site. In previous studies, imidazole was shown to restore cleavage activity in CRISPR endonucleases with a mutated active site histidine [27,35]. Therefore, we used the

Cas6-1 H51A mutant and imidazole supplemented cleavage buffer but could not restore Cas6-1 endoribonuclease activity.

We showed that *Synechocystis* Cas6-1 acts as a single turnover enzyme *in vitro* which was also observed for Cas6 enzymes from *Thermus thermophilus* and *Pseudomonas aeruginosa* [6,26,27]. These endoribonucleases presumably retain the processed substrate, which might point to an additional role of Cas6-1 further downstream of the Cas machinery, e.g., as part of the effector complex similar to type I-B, I-C, I-E and I-F

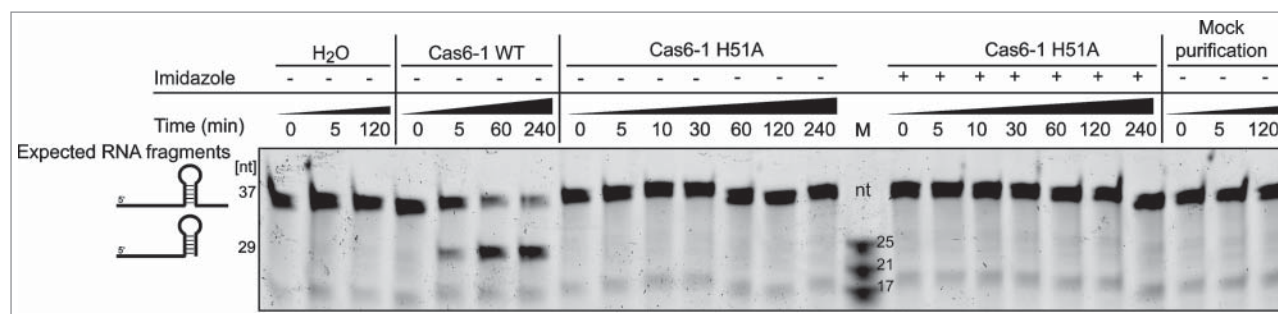


Figure 5. *In vitro* cleavage assay of the inactive Cas6-1 H51A mutant supplemented with imidazole. Imidazole was supplemented in *in vitro* cleavage assays to promote the recovery of endonuclease activity of the inactive Cas6-1 H51A mutant. The addition of imidazole to the cleavage buffer could not restore the catalytic activity of Cas6-1 H51A in comparison to the active WT enzyme. 500 mM imidazole was supplemented to samples marked with + imidazole in the cleavage buffer.

systems [5,6]. Persistent binding of Cas6-1 to the acrRNA after cleavage might result in the stabilization of cleavage intermediates and mature acrRNA and suggests a role of Cas6-1 in the interference complex, e.g., to facilitate or enable RNA-guided interference.

The CRISPR1 repeat substrate was cleaved *in vitro* by the Cas6-1 WT version at a rate of 0.04–0.06 min^{−1}. This is almost two orders of magnitude lower than the rate constants observed for the WT forms of other Cas6 and related CRISPR maturation enzymes. The observed rates of cleavage for the enzymes TtCas6A and TtCas6B of *Thermus thermophilus* HB8 were reported to be 3.2 and 3.7 min^{−1} [27]. Similar values were found for the *Pseudomonas aeruginosa* Cas6f (also called Csy4) with ~3 min^{−1} [38], the *S. solfataricus* Cas6-1 (3.69 min^{−1}) [39] or the *Thermus thermophilus* Cas6e (also called Cse3) with 4.9 min^{−1} [40]. By contrast, even slower cleavage rates were reported for mutated forms of the tested enzymes, for instance 0.0099 ± 0.0002 min^{−1} for the *Thermus thermophilus* H26A Cas6e mutant [40].

It is interesting that all these values are already several orders of magnitude slower than those of other well-characterized RNases, such as RNase A, which vary between values of 910 to 40500 min^{−1} [41], depending on the organism. While the exact reasons are not clear, it has been suggested that CRISPR maturation enzymes such as Csy4 evolved as RNA binding protein exhibiting highly accurate substrate selection while retaining only modest cleavage kinetics due to the lack of selection for rapid cleavage kinetics [38]. Therefore, the here reported findings for Cas6-1 of *Synechocystis* sp. PCC 6803 fit well to this overall picture.

We show that Cas6-1 is able to cleave acrRNA also *in vivo* in a strain lacking all other CRISPR1 associated proteins revealing it as an entirely autonomous entity regarding the first endoribonucleolytic processing step. However, secondary 3'-trimming of acrRNA intermediates was not observed and therefore depends on the presence of further CRISPR1 proteins that remain to be identified. In addition, it is not known whether these proteins have a function as adaptor to recruit a host ribonuclease or perform the 3'-trimming by themselves. It is worth mentioning that the 3'-trimming is accomplished by currently unknown mechanisms unrelated to Cas6 [5,42]. Interestingly, the two smallest cleavage fragments (30 and 39 nt in *in vivo* and 32 (+2 nt at the 5' end resulting from *in vitro* transcription) and 39 in *in vitro*) were only detectable in *in vitro* cleavage assays and absent in the *in vivo* situation. The 39 nt product

corresponds to the *oop* terminator and the 30/32 nt products encompass the 5' fragments of the first repeat. These short RNA fragments might be subject to degradation by host ribonucleases due to missing Cas6-1 binding or their abundance was below the detection limit. In contrast, the full-length acrRNA transcript and its intermediate cleavage products seem to remain stable within the cell, presumably stabilized by their secondary structures and by potentially associated proteins, e.g., Cas6-1.

In a homology-based model of Cas6-1 super-positioned over a *S. solfataricus* repeat RNA [19] crystal structure, amino acid positions of the Cas6-1 mutagenized conserved residues to the bound repeat RNA were analyzed. The positions of amino acids within the Cas6-1 model showing an effect on its enzymatic activity, especially H51, to the repeat RNA correlate well with the results obtained in *in vitro* and *in vivo* cleavage assays revealing residues located in close proximity to the repeat RNA as the same residues that exhibit destructive effects on Cas6-1 enzyme activity.

Materials and methods

Multiple sequence alignments of Cas6 proteins

Multiple sequence alignments were generated using the Clustal Omega web service with default settings [43]. Percent identity matrices were obtained from the result summary provided by Clustal Omega. Candidates for the alignment of uncharacterized cyanobacterial Cas6 proteins were selected by performing a BlastP search with the *Synechocystis* 6803 Cas6-1 protein sequence (UniProt-ID: Q6ZEI4) against the NCBI database.

Cloning, expression and purification of Cas6-1 endonuclease variants in *E. coli*

The gene *slr7014* that encodes Cas6-1 [28] and its mutagenesis variants were assembled in plasmid pQE70 (QIAGEN) and used for protein overexpression and purification in *E. coli* according to Reimann et al. [17]. Several mutations causing amino acid substitutions were introduced into *cas6-1* with the aid of the NEBaseChanger kit for site-directed mutagenesis (New England Biolabs). The Cas6-1 mutants differ in one to two amino acids from the wild-type version (R29A, H32A-S33A, H51A, R67A, R81A, K155A, R176A-R177A, K231A). The primers for mutagenesis (Table S1) were designed using

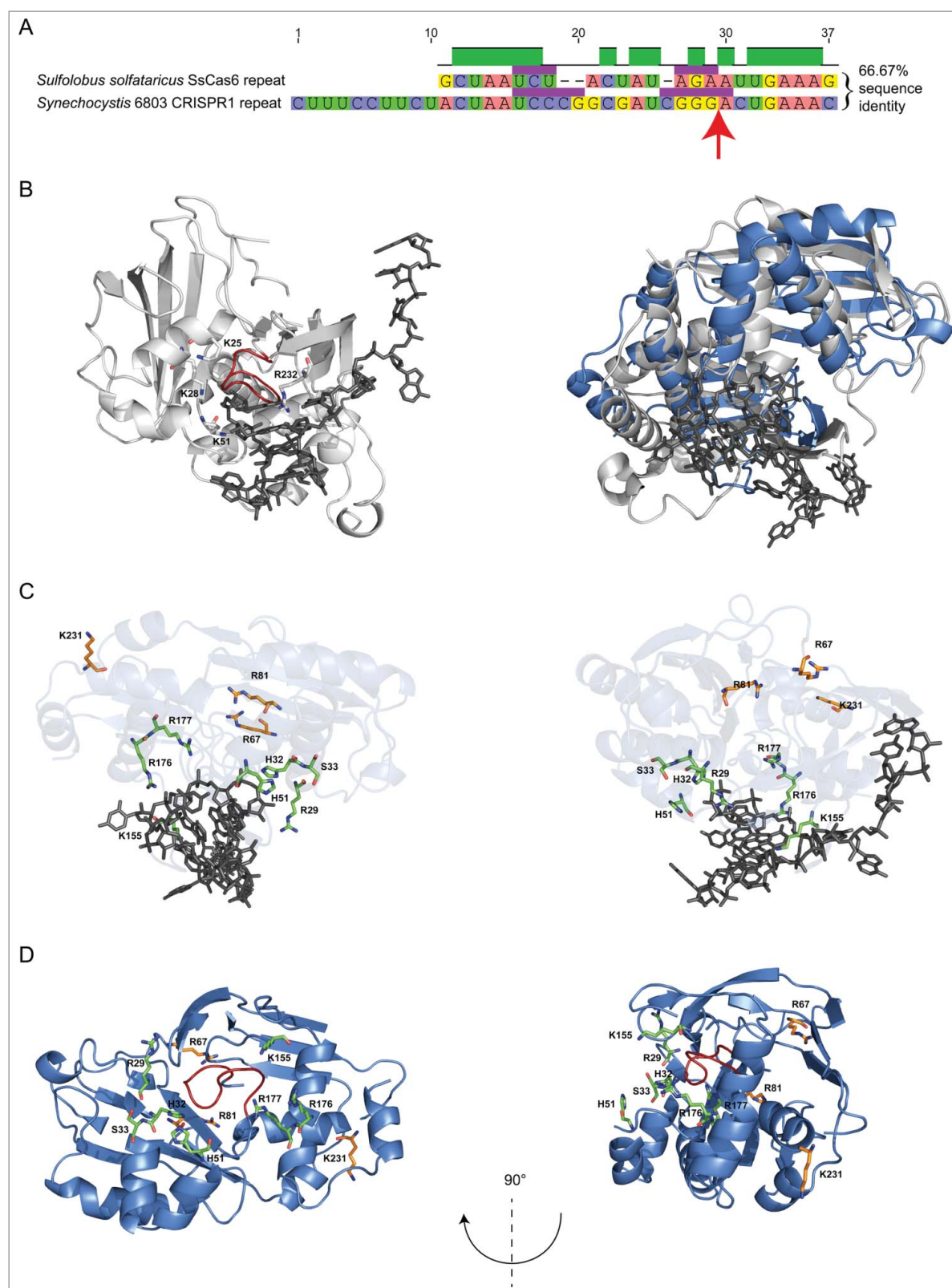


Figure 6. Homology-based model of Cas6-1 super-positioned over a *S. solfataricus* Cas6-1A (SsCas6)-crRNA cocrystal structure [19]. (A) Sequence alignment of the *S. solfataricus* and the *Synechocystis* 6803 CRISPR1 repeat sequences reveals a sequence identity of 66.67%. Nucleotides involved in stem loop formation and identical nucleotides are highlighted by a purple and green box above the nucleotide sequence, respectively. Cleavage sites of both CRISPR repeat sequences are indicated by red wedges. (B) Homology-based modelling of Cas6-1 super-positioned over the *S. solfataricus* repeat RNA crystal structure (grey) [19] reveals potential positions of the Cas6-1 amino acids relative to the bound repeat RNA (RMSD = 2.8). Positions of selected amino acids showing an impact (green) or no effect (orange) on Cas6-1 cleavage activity are displayed. The relative positions of amino acids to the repeat RNA indicated by this model are in good agreement with the results obtained in *in vitro* cleavage assays presented in Fig. 2B and C. (C) The glycine-rich-loop (red) – part of the C-terminal RNA recognition motif – also reaches inside a potential RNA-binding-pocket formed by the amino acids (green) that affect Cas6-1 (blue) cleavage activity. Amino acids without effects on Cas6-1 enzyme activity (orange) are positioned distantly from the potential RNA-binding-pocket indicating that these residues are not involved in the catalytic site or RNA binding of Cas6 and might have other functions instead.

the respective tool on the New England Biolabs website (<http://nebasechanger.neb.com/>). Divergent from the protocol provided in Reimann et al. [17], protein overexpression was performed in a culture volume of 500 mL, proteins were purified in a bed volume of 250 μ L Ni²⁺-NTA-agarose (QIAGEN) suspension and eluted protein fractions were concentrated using VivaspinTM 2 concentrators (GE Healthcare). Thereby the buffer was exchanged to PBS (140 mM NaCl, 2.7 mM KCl, 10 mM Na₂HPO₄, 1.8 mM KH₂PO₄; pH 7.3). Final protein concentrations were determined using the Qubit[®] Fluorometer (Thermo Fisher Scientific). Purified proteins were analyzed via sodium dodecyl sulphate-polyacrylamide (PAA) gel electrophoresis (SDS-PAGE) (6% PAA stacking gel, 15% PAA separating gel), visualized by InstantBlue Protein Stain (Expedeon) for 1 h, aliquoted and stored at -80°C until use.

Cloning, transformation and expression of Cas6-1 endonuclease variants in *Synechocystis* 6803

To analyze Cas6-1 enzyme activity *in vivo*, the entire CRISPR1 locus was deleted by integrating a kanamycin resistance cassette into the corresponding locus. The resulting *Synechocystis* Δ C1 strain is devoid of the respective *cas* genes and the corresponding CRISPR repeat-spacer array. The up- and downstream flanking regions (1,200 and 1,800 bp in size) were amplified via PCR to ensure site-directed integration via homologous recombination. The resistance cassette in vector pUC19 was placed in between the upstream and downstream flanking regions by Gibson assembly [44]. Transformation of 10 mL *Synechocystis* 6803 aliquots was performed as described [31]. Transformants were tested for full segregation of the introduced knock-out (KO) via PCR screening. *Synechocystis* 6803 cultures were grown as described [39]. For controllable overexpression of Cas6-1 in *Synechocystis* 6803, the *slr7014* WT and mutagenesis sequences were fused to the copper-inducible P_{petE} [32,33] and downstream of the Cas6-1 expression cassette to the bacteriophage λ *oop* terminator and a streptomycin resistance cassette. The PCR fragment was subcloned in pUC19 containing the identical up- and downstream flanking regions used for the creation of the Δ C1 KO strain and transformed in Δ C1 *Synechocystis* 6803 using appropriate antibiotics. For induction, *Synechocystis* 6803 strains were grown to an OD₇₅₀ of 0.6–0.8 and Cas6-1 protein expression and acrRNA expression were induced by adding 1.5 μ M CuSO₄ and 2.5 μ M ZnSO₄ to the growth medium, respectively.

Design and construction of the artificial CRISPR RNA

We designed two artificial spacers with a length of 36 nt because native CRISPR1 spacers vary between 31 and 41 nucleotides in size [31]. As suitable endogenous targets, the *cpcBA* mRNA was selected encoding α and β phycocyanin.

Beginning at position -21 up to position -1 with regard to the *cpcB/A* start codon, four potential spacer sequences with 5 nt increment each were determined spanning over different portions of the mRNAs, containing parts of the respective 5'UTRs, the start codons and successive nucleotides within the reading frames of *cpcB* and *cpcA*. To minimize off-target effects, the spacer sequences exhibiting the lowest combined energy

score, predicted by IntaRNA [45], were selected. The finally selected sequences cover positions -16 to $+20$ within the *cpcB* mRNA (acrRNA1) and -6 to $+30$ within the *cpcA* mRNA (acrRNA2). Spacer-repeat interactions can disturb proper recognition by the Cas6 maturation endonucleases [17]. Therefore, we minimized the theoretically possible interactions to a maximum of 5 (acrRNA1) and 7 (acrRNA2) consecutive complementary nucleotides and predicted interaction energies of -12.6 kcal/mol between acrRNA1 and the CRISPR repeat and -19.6 kcal/mol for acrRNA2 as predicted by RNAhybrid [46]. The repeat-spacer array was subject to gene synthesis by Eurofins. The zinc responsive promoter P_{ziaA} [34] was added upstream of the coding sequence by Gibson assembly [44] to achieve inducible expression. The *oop* terminator was attached at the 3' end of the repeat-spacer array to ensure efficient transcription termination. The construct was assembled in a *Xba*I/*Xho*I digested pVZ321 vector via Gibson assembly, resulting in the following construct: Zn²⁺-inducible promoter *ziaA* (including the *ziaR* sequence, -10 element and the transcription start site; the 5'UTR of the native *ziaA* was omitted), CRISPR1 repeat, anti-*cpcB* spacer, CRISPR1 repeat, anti-*cpcA* spacer, CRISPR1 repeat, *oop* terminator. The cloned fragments were verified by DNA sequencing (GATC Biotech).

Synechocystis 6803 conjugation

The acrRNA containing conjugative plasmid pVZ321 was conjugated into *Synechocystis* 6803 containing Cas6-1 WT and mutagenized Cas6-1 variants by triparental mating as previously described [28]. Briefly, overnight cultures of the helper strain *E. coli* J53/RP4 and the donor strain *E. coli* DH5 α with the plasmid of interest were combined and incubated for 1 h at 30°C without shaking. *Synechocystis* 6803 cultures (OD₇₅₀ 0.6–0.8) were harvested, resuspended in BG11 and combined with the mixed culture of the plasmid-bearing and helper culture. The pellet was resuspended in BG11 and placed on a sterile filter. After an overnight incubation at 30°C with slightly covered plates, the filter was rinsed with BG11 and the resulting cell suspension was plated on BG11 agar plates containing appropriate antibiotics and incubated at 30°C for approximately 2 weeks.

RNA analysis and hybridization conditions

RNA extraction from 50 mL *Synechocystis* 6803 cultures was performed as described [31] with the following variations. Cells were collected by centrifugation in a swing-out rotor (Beckman Coulter Allegra X-12, 3,500 rpm at room temperature). Pellets were resuspended in 1 mL PGTX and incubated for 15 min at 65°C . RNA pellets were washed with 75% EtOH. Ten micrograms of total RNA per lane were separated on PAA-urea gels (10% PAA, 0.5 g/mL urea, 1 \times Tris-Borate-EDTA (TBE) buffer) and electroblotted onto Hybond N+ membranes (Amersham). RNA was cross-linked to the membrane at 120 mJ/cm² for 1.5 min. Membranes were prehybridized for 10 to 60 min at 62°C with hybridization buffer (50% deionized formamide, 7% SDS, 250 mM NaCl, and 120 mM NaPi buffer, pH 7.2) in glass tubes under continuous rotation. Transcript probes for northern hybridization were generated by *in vitro* transcription from PCR amplified templates using the Ambion

MAXIscrip kit with 50-fold-reduced UTP concentration and 50 μCi ^{32}P -UTP. The reactions were incubated at 37°C for 10 min, then supplemented with 1 μL DNase (2U/ μL) and incubated for an additional 15 min at 37°C to remove the DNA templates. Reactions were stopped by the addition of 1 μL 0.5 M EDTA (pH 8.0), secondary structures denatured at 80 to 90°C for 5 min, kept on ice for 2 min and then added to the prehybridized membranes for hybridization at 62°C overnight. Membranes were washed at 57°C with washing solutions I (2 \times SSC and 1% SDS), II (1 \times SSC and 0.5% SDS) and III (0.1 \times SSC and 0.1% SDS) for 10 min each. The signals were detected with a storage phosphor screen (Kodak) and a GE Typhoon FLA 9500 imaging system.

In vitro transcription and purification

The pre-acrRNA transcript was generated via *in vitro* transcription according to Reimann et al. [17] and subjected to gel purification. Primer sequences for preceding PCR amplifications are provided in Table S1.

RNase cleavage assays with synthetic oligonucleotides or in vitro transcripts

Cleavage assays were conducted according to Reimann et al. [17] with the following variations. The reactions were performed in buffer B (cleavage buffer) with 500 nM acrRNA *in vitro* transcript or CRISPR1 repeat oligonucleotides (Table S1) and 62.5 – 500 nM purified Cas6-1 endonuclease at 30°C. Negative controls were complemented with 1 μL of H₂O or 1 μL eluate of a mock purification with cells harboring the respective plasmid (pQE70) without any inserted gene (mock control). To determine the cleavage rate constant k_{cl} of a first order reaction 500 nM CRISPR1 repeat were incubated in different ratios with Cas6-1 (2:1, 4:1, 8:1 with 1 μM , 2 μM and 4 μM enzyme) for indicated time points up to 15 min. Fractions of substrate and product were determined from the gel images using Quantity One software (BIO-RAD). The fraction of uncleaved substrate RNA was calculated by dividing the amount of substrate by the sum of the amount of product and substrate. Substrate fractions were plotted against time in an exponential decay curve according to the equation $A_t = A_0 \cdot \exp(-k_{\text{cl}} \cdot t)$ where A is the fraction of uncleaved substrate at time point t and k_{cl} is the first order rate constant of cleavage. The natural logarithm of the determined substrate fractions was plotted against time according to the linear equation $\ln(A_t) = -k_{\text{cl}} \cdot t + \ln(A_0)$ with k_{cl} as the negative slope. k_{cl} was specified as average of three independently performed experiments. To test whether the catalytic activity of the Cas6-1 H51A mutant can be restored, the cleavage buffer was supplemented with 500 mM imidazole, pH 8.0 and either pre-incubated at 4°C overnight or directly transferred to 30°C. The low range ssRNA ladder (ssRNA marker) (New England Biolabs), the RiboRuler low range RNA ladder (Thermo Fisher Scientific) and the microRNA marker (New England Biolabs) served as RNA ladders for size estimation. The CRISPR1 repeat oligo ladder (C1L) was generated by alkaline hydrolysis (50 mM Tris-HCl pH 8.5,

20 mM MgCl₂) with 25 pmol substrate and was incubated for 72 h to 96 h at 30°C.

Disclosure of potential conflicts of interest

No potential conflicts of interest were disclosed.


Acknowledgements

We thank Sonja Albers and Chris van der Does for their support with the PyMol analysis.

Funding

Financial support for this work by the German Research Foundation (DFG) program FOR1680 “Unravelling the Prokaryotic Immune System” (grant HE 2544/8-2) to WRH is greatly acknowledged.

ORCID

Wolfgang R. Hess  <http://orcid.org/0000-0002-5340-3423>

References

- [1] Jansen R, van Embden JDA, Gaastra W, et al. Identification of genes that are associated with DNA repeats in prokaryotes. *Mol Microbiol.* 2002;43:1565–75.
- [2] Lange SJ, Alkhnbashi OS, Rose D, et al. CRISPRmap: an automated classification of repeat conservation in prokaryotic adaptive immune systems. *Nucleic Acids Res.* 2013;41:8034–44.
- [3] Bhaya D, Davison M, Barrangou R. CRISPR-Cas systems in Bacteria and Archaea: versatile small RNAs for adaptive defense and regulation. *Annu Rev Genet.* 2011;45:273–97.
- [4] Grissa I, Vergnaud G, Pourcel C. The CRISPRdb database and tools to display CRISPRs and to generate dictionaries of spacers and repeats. *BMC Bioinformatics.* 2007;8:172.
- [5] Hochstrasser ML, Doudna JA. Cutting it close: CRISPR-associated endoribonuclease structure and function. *Trends Biochem Sci.* 2015;40:58–66.
- [6] Makarova KS, Wolf YI, Alkhnbashi OS, et al. An updated evolutionary classification of CRISPR-Cas systems. *Nat Rev Microbiol.* 2015;13:722–36.
- [7] Westra ER, Dowling AJ, Broniewski JM, et al. Evolution and ecology of CRISPR. *Annu Rev Ecol Evol Syst.* 2016;47:307–31.
- [8] Koonin EV, Makarova KS, Wolf YI. Evolutionary genomics of defense systems in Archaea and Bacteria. *Annu Rev Microbiol.* 2017;71:233–261.
- [9] Hale C, Kleppe K, Terns RM, et al. Prokaryotic silencing (psi)RNAs in *Pyrococcus furiosus*. *RNA.* 2008;14:2572–9.
- [10] Hale CR, Zhao P, Olson S, et al. RNA-guided RNA cleavage by a CRISPR RNA-Cas protein complex. *Cell.* 2009;139:945–56.
- [11] Karginov FV, Hannon GJ. The CRISPR system: small RNA-guided defense in Bacteria and Archaea. *Mol Cell.* 2010;37:7–19.
- [12] Przybilski R, Richter C, Gristwood T, et al. Csy4 is responsible for CRISPR RNA processing in *Pectobacterium atrosepticum*. *RNA Biol.* 2011;8:517–28.
- [13] Nam KH, Haitjema C, Liu X, et al. Cas5d protein processes pre-crRNA and assembles into a cascade-like interference complex in subtype I-C/Dvulg CRISPR-Cas system. *Struct.* 1993; 2012;20:1574–84.
- [14] Punetha A, Sivathanu R, Anand B. Active site plasticity enables metal-dependent tuning of Cas5d nuclease activity in CRISPR-Cas type I-C system. *Nucleic Acids Res.* 2014;42:3846–56.
- [15] Zetsche B, Gootenberg JS, Abudayyeh OO, et al. Cpf1 is a single RNA-guided endonuclease of a class 2 CRISPR-Cas system. *Cell.* 2015;163:759–71.

- [16] Abudayyeh OO, Gootenberg JS, Konermann S, et al. C2c2 is a single-component programmable RNA-guided RNA-targeting CRISPR effector. *Science*. 2016;353:aaf5573.
- [17] Reimann V, Alkhnbashi OS, Saunders SJ, et al. Structural constraints and enzymatic promiscuity in the Cas6-dependent generation of crRNAs. *Nucleic Acids Res*. 2017;45:915–25.
- [18] Lintner NG, Kerou M, Brumfield SK, et al. Structural and functional characterization of an archaeal clustered regularly interspaced short palindromic repeat (CRISPR)-associated complex for antiviral defense (CASCADE). *J Biol Chem*. 2011;286:21643–56.
- [19] Shao Y, Li H. Recognition and cleavage of a nonstructured CRISPR RNA by its processing endoribonuclease Cas6. *Structure*. 2013;21:385–93.
- [20] Sokolowski RD, Graham S, White MF. Cas6 specificity and CRISPR RNA loading in a complex CRISPR-Cas system. *Nucleic Acids Res*. 2014;42:6532–6541.
- [21] Richter H, Zoephel J, Schermuly J, et al. Characterization of CRISPR RNA processing in *Clostridium thermocellum* and *Methanococcus maripaludis*. *Nucleic Acids Res*. 2012;40:9887–96.
- [22] Wang R, Preamplume G, Terns MP, et al. Interaction of the Cas6 ribonuclease with CRISPR RNAs: recognition and cleavage. *Structure*. 2011;19:257–64.
- [23] Brouns SJJ, Jore MM, Lundgren M, et al. Small CRISPR RNAs guide antiviral defense in prokaryotes. *Science*. 2008;321:960–4.
- [24] Makarova KS, Haft DH, Barrangou R, et al. Evolution and classification of the CRISPR–Cas systems. *Nat Rev Microbiol*. 2011;9:467–77.
- [25] Haurwitz RE, Jinek M, Wiedenheft B, et al. Sequence- and structure-specific RNA processing by a CRISPR endonuclease. *Science*. 2010;329:1355–8.
- [26] Haurwitz RE, Sternberg SH, Doudna JA. Csy4 relies on an unusual catalytic dyad to position and cleave CRISPR RNA. *EMBO J*. 2012;31:2824–32.
- [27] Niewoehner O, Jinek M, Doudna JA. Evolution of CRISPR RNA recognition and processing by Cas6 endonucleases. *Nucleic Acids Res*. 2014;42:1341–53.
- [28] Scholz I, Lange SJ, Hein S, et al. CRISPR-Cas systems in the cyanobacterium *Synechocystis* sp. PCC6803 exhibit distinct processing pathways involving at least two Cas6 and a Cmr2 protein. *PLoS ONE*. 2013;8:e56470.
- [29] Behler J, Sharma K, Reimann V, et al. The host-encoded RNase E endonuclease as the crRNA maturation enzyme in a CRISPR-Cas subtype III-Bv system. *Nat Microbiol*. 2018;3:367–77.
- [30] Sefcikova J, Roth M, Yu G, et al. Cas6 processes tight and relaxed repeat RNA via multiple mechanisms: A hypothesis. *BioEssays News Rev Mol Cell Dev Biol*. 2017;39.
- [31] Hein S, Scholz I, Voß B, et al. Adaptation and modification of three CRISPR loci in two closely related cyanobacteria. *RNA Biol*. 2013;10:852–64.
- [32] Zhang L, McSpadden B, Pakrasi HB, et al. Copper-mediated regulation of cytochrome c553 and plastocyanin in the cyanobacterium *Synechocystis* 6803. *J Biol Chem*. 1992;267:19054–9.
- [33] Briggs LM, Pecoraro VL, McIntosh L. Copper-induced expression, cloning, and regulatory studies of the plastocyanin gene from the cyanobacterium *Synechocystis* sp. PCC 6803. *Plant Mol Biol*. 1990;15:633–42.
- [34] Thelwell C, Robinson NJ, Turner-Cavet JS. An SmtB-like repressor from *Synechocystis* PCC 6803 regulates a zinc exporter. *Proc Natl Acad Sci USA*. 1998;95:10728–33.
- [35] Lee HY, Haurwitz RE, Apffel A, et al. RNA-protein analysis using a conditional CRISPR nuclease. *Proc Natl Acad Sci USA*. 2013;110:5416–21.
- [36] Carte J, Wang R, Li H, et al. Cas6 is an endoribonuclease that generates guide RNAs for invader defense in prokaryotes. *Genes Dev*. 2008;22:3489–96.
- [37] Gesner EM, Schellenberg MJ, Garside EL, et al. Recognition and maturation of effector RNAs in a CRISPR interference pathway. *Nat Struct Mol Biol*. 2011;18:688–92.
- [38] Haurwitz RE, Sternberg SH, Doudna JA. Csy4 relies on an unusual catalytic dyad to position and cleave CRISPR RNA. *EMBO J*. 2012;31:2824–32.
- [39] Sokolowski RD, Graham S, White MF. Cas6 specificity and CRISPR RNA loading in a complex CRISPR-Cas system. *Nucleic Acids Res*. 2014;42:6532–41.
- [40] Sashital DG, Jinek M, Doudna JA. An RNA-induced conformational change required for CRISPR RNA cleavage by the endoribonuclease Cse3. *Nat Struct Mol Biol*. 2011;18:680–7.
- [41] Katoh H, Yoshinaga M, Yanagita T, et al. Kinetic studies on turtle pancreatic ribonuclease: a comparative study of the base specificities of the B2 and P0 sites of bovine pancreatic ribonuclease A and turtle pancreatic ribonuclease. *Biochim Biophys Acta*. 1986;873:367–71.
- [42] Li H. Structural principles of CRISPR RNA processing. *Struct*. 2015;23:13–20.
- [43] McWilliam H, Li W, Uludag M, et al. Analysis tool web services from the EMBL-EBI. *Nucleic Acids Res*. 2013;41:W597–600.
- [44] Gibson DG, Young L, Chuang R-Y, et al. Enzymatic assembly of DNA molecules up to several hundred kilobases. *Nat Methods*. 2009;6:343–5.
- [45] Wright PR, Georg J, Mann M, et al. CopraRNA and IntaRNA: predicting small RNA targets, networks and interaction domains. *Nucleic Acids Res*. 2014;42:W119–123.
- [46] Rehmsmeier M. Prediction of microRNA targets. *Methods Mol Biol*. 2006;342:87–99.